

RSC Advances



This is an *Accepted Manuscript*, which has been through the Royal Society of Chemistry peer review process and has been accepted for publication.

Accepted Manuscripts are published online shortly after acceptance, before technical editing, formatting and proof reading. Using this free service, authors can make their results available to the community, in citable form, before we publish the edited article. This *Accepted Manuscript* will be replaced by the edited, formatted and paginated article as soon as this is available.

You can find more information about *Accepted Manuscripts* in the [Information for Authors](#).

Please note that technical editing may introduce minor changes to the text and/or graphics, which may alter content. The journal's standard [Terms & Conditions](#) and the [Ethical guidelines](#) still apply. In no event shall the Royal Society of Chemistry be held responsible for any errors or omissions in this *Accepted Manuscript* or any consequences arising from the use of any information it contains.

Enhancing Damping Properties of Epoxy Resins Using Silicone Macromolecules Intercalated Montmorillonite Clay

Chen Yang, Yao Dingyang, Zou Huawei¹, Liang Mei¹

(The State Key Lab. of Polymer Materials Engineering, Polymer Research Institute of
Sichuan University, Chengdu 610065, China)

Abstract: In this paper, the possibility of improving the damping properties of epoxy resin through dispersion of silicone-intercalated organic montmorillonite was investigated. Flexible silicone macromolecules were inserted into organo-modified montmorillonite (OMMT) by an intercalation to prepare a layered structure that similar to a constrained layer damping structure unit. The effects of silicone macromolecule type, weight ratio of silicone/OMMT and solvent for the intercalation on the structure and properties of the composites were studied by X-ray diffraction (XRD), dynamic mechanical analysis (DMA), and transmission electron microscopy (TEM). The influence of the silicone-intercalated OMMT with different content on the damping properties of the materials was also investigated. The damping property of the final, cured materials was probed using DMA. Analysis of XRD and TEM proved that the silicone-intercalated OMMT had been successfully prepared under an appropriate process. The presence of the silicone-intercalated OMMT decreased the glass transition temperature (T_g) of the epoxy, and the epoxy-nanocomposites achieved a better damping performance.

Keywords: montmorillonite, damping materials, inserted layer structure, epoxy resin,

¹ Corresponding author Tel: +86-28-85408288; Fax: +86-28-85402465. E-mail address: hwzou@163.com (Zou Huawei) or liangmeiww@163.com (Liang Mei)

silicone

1. Introduction

Epoxy resin is a matrix with excellent physical and chemical properties after curing, and is widely used in the field of composite materials. However, most epoxy systems with high modulus and tensile strength exhibit a high glass transition temperature which corresponds to the maximum loss factor of a polymeric material. Many authors have reported on high performance vibration absorbers that demonstrate a high loss factor over a wide temperature range. Several ways of improving the damping properties of an epoxy have been shown as follows: 1) Polymer blend modification, which is the most common way to broaden the range of Tg. Yamada and Shoji ^[1] investigated a ternary blend based on poly(vinyl chloride), chlorinated polyethylene, and epoxidized natural rubber. They found that suitable compositions could yield good mechanical properties and high loss factor over a wide temperature and frequency range. 2) Filler addition, which can result in mechanical damping contributed from three aspects ^[2]: internal friction among the macromolecules, interaction between macromolecules and fillers and mutual friction among fillers. Huang and Zhan ^[3] studied the dynamic mechanical and vibration damping properties of polyether urethane and epoxy composites. According to their research, adding a planar filler increased the shear motion and the internal dissipation in polyurethane (PU) materials. 3) Interpenetrating polymer networks ^[4-6], which is a form of polymer blends developed first in the 1960s. The Tg of an epoxy resin can be lowered by introducing flexible chains in the interpenetrating networks. The achieved

material is often used as coatings. However, to obtain a kind of structural material, polymer/layered silicate (PLS) nanocomposites based on epoxy resin were prepared [7-8].

In recent years PLS nanocomposites have attracted a considerable research interest, both in industry and in academia [9]. As a kind of new material, PLS nanocomposites exhibit remarkable improvement in such properties as strength, heat resistance [10], flammability [11] and biodegradability of biodegradable polymers [12]. Depending on the strength of interfacial interaction between the polymer matrix and the layered silicate, three different types of PLS nanocomposites can be achieved [9]: intercalated nanocomposites, flocculated nanocomposites and exfoliated nanocomposites.

The aim of the research described here was to obtain structural and damping integration nanocomposites. The desired micro-constrained layer damping structure unit is illustrated in Fig.1. The constrained layer damping configuration is a type of sandwich structure, which is composed of the substrate, a damping layer, and a second constrained layer. The damping layer is a viscoelastic layer while the constrained layer is a stiff layer. It yields better damping than the extensional type due to the shear motion between the damping layer and the constrained layer. [13-14] In our work, the flexible silicone macromolecule acts as the damping layer while the organo-modified montmorillonite acts as the constrained layer, which is expected to achieve a composite with good damping performance in a wide temperature range.

2. Experimental

2.1 Materials

Two kinds of clays were used in our research. One was a commercially available octadecyl ammonium ion-modified montmorillonite layered silicate from Nanocor. (Nanomer I.30P, USA), with an interlayer d-space of 2.3 nm, named as OMMT. The other was an organic montmorillonite prepared in our laboratory, modified by hexadecyl trimethyl ammonium bromide ^[15], with an interlayer d-space of 2.4 nm, named as self-made OMMT, and SOMMT for short. The hydroxyl silicone oils, named as hydroxyl silicone of high viscosity (HVHS) and hydroxyl silicone oil of low viscosity (LVHS), were purchased from Chenguang Research Institute of Chemistry (China), having a kinematic viscosities of 3000cSt (hydroxyl content: 0.08%, Mw=40000g/mol) and 30cSt (hydroxyl content: 8%, Mw=900g/mol), respectively. Another phenyl silicone oil, named as phenyl silicone oil of low viscosity (LVPS), was purchased from Qiaorui Co.Ltd (China), having a kinematic viscosity of 30cSt (phenyl content: 25%, Mw=1200g/mol). The epoxy resin (EP) used as the polymer matrix was supplied by Wuxi Resin Factory (China), offering epoxide equivalent weight of 196, viscosity of 12 Pa.s. The curing agent was diamino diphenyl methane (DDM), and was purchased from Shanghai SSS Reagent Co. (China).

2.2 Preparation of silicone-intercalated organo-modified montmorillonite

For the synthesis of silicone-intercalated organo-modified montmorillonite, two preparative methods, solution intercalation and melt intercalation, were employed. For solution intercalation, organo-modified montmorillonite was dispersed in solvent by mechanical stirring at 300 rpm at 20°C for 30 min. Then, the silicone macromolecules

was added into the mixture and mechanical stirring at 300 rpm continued at 60°C for 9 h. Finally, the resulting slurry was dried in a small flask at 120°C. The melt intercalation method, was environmentally benign due to the absence of organic solvent. For this method, the silicone macromolecules and organo-modified montmorillonite were mixed in a beaker by mechanical stirring at 400 rpm at 60°C for 90 min to complete the intercalation. In contrast to the intercalated OMMT, we prepared the un-intercalated OMMT by blending the OMMT and LVPS (or LVHS) by mechanical stirring at 300 rpm at 60°C for 2 min.

2.3 Preparation of epoxy-nanocomposites

A certain percent of silicone-intercalated organic montmorillonite and epoxy resin were weighed in a beaker. Then, the melt DDM were added and the blend were mixed on a three roll mill for 30 minutes at 20°C . The blend was poured into a mold after heating at 60°C under vacuum to eliminate air bubbles. The blend was cured for 2h at 135°C and 2h at 175°C.

2.4 Characterization

Wide-angle X-ray diffraction (XRD) analysis were performed on Philips X-ray DY-1291 diffractometer (Netherlands). An acceleration voltage of 40 kV and a current of 35 mA were applied using Ni filtered Cu Ka radiation.

The loss factor, $\tan \delta$, of the nanocomposites was determined using a DMA-Q800 (TA Instruments Co., USA). The cured samples were clamped in a medium frame using a small center clamp in the three-point bending mode. The test was performed from 100°C to 220°C at a ramp of 3°C/min using a frequency of 1Hz.

The samples were rectangular bars of sizes 30 mm×10 mm×4 mm.

Transmission electron microscopy (TEM) was undertaken using a Tecnai-G²F20 instrument (FEI Corporation, USA) at 120 kV to observe the silicate structure in the nanocomposites. The ultrathin sections with a thickness of 100 nm were cryogenically microtomed by an ultra-microtome (EM UC7, LEICA, Germany).

3. Results and discussion

3.1 Characterization of the silicone-intercalated organo-modified montmorillonite

It was very important to choose an appropriate solvent when we prepared the silicone-intercalated organo-modified montmorillonite by solution intercalation. Figure 2 shows the XRD patterns of HVHS-SOMMT with a weight ratio of 3:1 in different solvents. As shown in the figure, the diffraction pattern of the HVHS/SOMMT (flexible structure units) prepared in tetrahydrofuran (THF) had the characteristic (001) diffraction peak at 2.98° corresponding to a basal interlayer spacing, d , calculated as $\lambda/2\sin\theta$, equal to 3.0 nm, where λ is the X-ray wavelength and θ is the scattering angle. As for the HVHS-SOMMT, this peak shifted to a lower scattering vector, indicating an enlargement of the SOMMT gallery between the silicate layers. However, the location of diffraction peak of the flexible structure units prepared in chloroform did not change. The flexible structure units prepared in toluene (PT) and xylene (PX) exhibited peaks at 3.40° and 3.62°, corresponding to the basal interlayer spacing of 2.6 nm and 2.4 nm, respectively. It means that the SOMMT was intercalated by HVHS in THF more effectively than the other three solvents. Figure 3 shows the XRD patterns of HVHS-OMMT with a weight ratio of 3:1 in

different solvents. From Fig.3 similar conclusion was obtained as for Fig.2, that the interlayer spacing of OMMT had been enlarged by the intercalation of HVHS in THF. The thermodynamics involved in the solution intercalation are described according to the following formula:

$$\Delta G = \Delta H - T\Delta S \quad (1)$$

where ΔG is the variation in the Gibbs free energy, T is the temperature of the reaction and ΔH and ΔS are the variations in the enthalpy and entropy, respectively. For the overall process, in which HVHS is exchanged with the previously intercalated solvent in the interlayer, a negative variation in the Gibbs free energy is required. The driving force for the HVHS intercalation into layered silicate from solution is the entropy gained by desorption of solvent molecules, which compensates for the confined, intercalated polymer chains.^[16] According to the thermodynamics, additional entropy had been gained by the stronger solvation effect on the organic cations of OMMT or SOMMT by the polarity of THF. Therefore, THF was more effective than the other solvents. In addition, XRD analysis of PT and PX revealed a broad diffraction peak which showed the formation of a disordered intercalated structure. It can be conjectured that some layers of OMMT had been inserted by the smaller silicone macromolecules. This may be due to the solubility parameter of the silicone macromolecules and PT or PX is much closer, and the dissolution of the silicone macromolecules in PT or PX leads to this tiny intercalation. In Figs.2 and 3, the diffraction peak that appears at about 12° is a diffuse scattering peak of the silicone macromolecules.

The type of silicone macromolecule also has impact on the intercalation. Figure

4 shows that LVHS can achieve intercalation by solution intercalation in all solvents used, and the interlayer spacing was enlarged to 3.4 nm. Shorter silicon chains brought about higher density of chain terminals, which means more free volume than in case of longer silicon chains and were more likely to intercalate into the clay interlayers. Another difference between the diffraction patterns of HVHS-OMMT and LVHS-OMMT was that a new diffraction peak, which did not appear in Figs.2 and 3, was seen in Fig 4. This peak observed around 5° correlates to the (002) plane and it indicates that the coherent orders of the silicate layers in LVHS-OMMT were higher than that in HVHS-OMMT.^[17-18]

After the comparison above, THF was chosen as the solvent to prepare the silicone-intercalated organo-modified montmorillonite (named flexible structure units). Flexible structure units with different weight ratios of HVHS/ SOMMT were prepared. The XRD patterns in Fig. 5 show a steady decrease of peak height with the incremental content of silicone macromolecules. However, a similar d-spacing of SOMMT was detected at about 2.8 nm. It means that there was no significant effect on the intercalation by the weight ratio of HVHS / SOMMT in the preparation.

Melt intercalation is environmentally benign due to the absence of organic solvents, so we investigated the possibility of preparing silicone-intercalated OMMT by this method. When preparing the flexible units by melt intercalation, LVHS and LVPS were chosen as matrices for their low viscosity of the blend could make the intercalation more easily. The silicone macromolecules with small chains were intercalated into the interlayers of OMMT because the d-spacing of the interlayers

was nearly 3.2 nm (Fig.6). XRD analysis of LVPS-OMMT reveals a broad diffraction peak which shows the formation of a disordered intercalated structure. This may be due to the introduction of phenyl side groups could destroy the regularity of the OMMT.

Flexible structure units with different weight ratios of LVHS/OMMT were prepared by the melt intercalation method. It can be observed from Fig.7 that the weight ratio of LVHS/OMMT in the preparation had no significant effect on the intercalation.

Figure 8-9 show the TEM morphology of the epoxy-nanocomposites with a LVHS-OMMT and LVPS-OMMT content of 15%, respectively. These two flexible structure units were prepared by melt intercalation at a ratio of 7:3 at 60°C for 90min. A multilayered silicate structure was seen in the nanocomposites. According to the XRD results, some of the flexible silicone macromolecules had been inserted into OMMT and the d-spacing of the interlayers was about 5 nm in the TEM which means some macromolecules of EP were also intercalated. It can be concluded that the constrained layer damping structure had been successfully prepared in the nanocomposites.

3.2 DMA analysis of epoxy-nanocomposites

Dynamic mechanical analysis (DMA) was applied to investigate the influence of the silicone-intercalated OMMT on the tan delta of the composites, which was used to characterize the damping performance of the epoxy-nanocomposites. In contrast to the intercalated OMMT, we prepared a composite by blending the OMMT and LVPS

(or LVHS) without an intercalation, named as blend OMMT. From Figs. 10-11 we can know that the material with silicone-intercalated OMMT has better damping performance than the material with blend OMMT, for the peak area of its loss factor was larger (Tab.1). Thus we can conclude that the constrained damping structure units of LVPS-OMMT or LVHS/OMMT improved the damping performance of the epoxy. In addition, un-intercalated silicone oil plasticization and a lower crosslink density of epoxy were also contributing to the decrease in T_g .

Figure 12a shows the comparison of the damping performance of the material with HVHS-OMMT and LVHS-OMMT. The peak area of loss factor of the epoxy-nanocomposites with LVHS-OMMT was larger than that with HVHS-OMMT. Shorter silicon chains bring about higher density of chain terminals, which means more free volume than longer silicon chains and are more likely to intercalate into the clay interlayers. Figure 12b shows the comparison of the damping performance of the material with HVPS-OMMT and LVPS-OMMT, and it shows the similar result to that in Fig.12a. But the material with LVPS-OMMT achieved a better damping performance when compared with the material with LVHS-OMMT. This may be due to the existence of the single phenyl in silicone chains which enhanced the friction between the polymer and the clay.

A series of epoxy-nanocomposites containing 0, 2, 4, 6 (wt%) LVHS-OMMT were prepared. The damping performance of material improved with increasing flexible structure unit concentration (Fig.13, Table.1). A tiny fluctuation of T_g was exhibited among the epoxy-nanocomposites with different content of LVHS-OMMT

in Fig.13. It has been reported that the addition of the organoclay can increase T_g by strengthening the polymer network by the polymer absorbed on the surface of the filler (increase of entanglements)^[19-20], while the free flexible silicone macromolecules can decrease it. These two factors, which provide the opposite effect, may account for the tiny fluctuation in T_g .

Figure14 shows that the epoxy-nanocomposites containing 15% LVHS-OMMT, when prepared by melt intercalation caused the glass transition temperature of EP to decrease but the peak area of the loss factor increase (Table.1). It is obvious that the introduction of flexible structure unit improves the damping properties over a wide temperature range, for example,the temperature range of $\tan \delta \geq 0.2$ for EP was 182.3°C to 197.6°C. However, the temperature range of $\tan \delta \geq 0.2$ was 160.6°C to 189.8°C for LVHS:OMMT=7:3 and 153.6°C to 187.5°C for LVHS:OMMT=8:2, respectively. Thus the two epoxy-nanocomposites achieved a better damping performance in a broader temperature range. The difference between the two curves illustrates that more flexible silicone macromolecules contributed to the lower glass transition temperature and more organoclay contributed to the higher peak of the loss factor. The decrease in T_g was due to the lack of surrounding entanglements caused by the free flexible macromolecules, while the increase of organoclay concentration meant a larger amount of constrained layer damping structure units which can cause the absorption of mechanical vibration energy.

4. Conclusion

Comparison of XRD analysis of the silicone macromolecule-intercalated OMMT

prepared by solution intercalation and melt intercalation showed that silicone macromolecules with lower molecular weight are more likely to form intercalated structures. The HVHS was able to achieve intercalation in tetrahydrofuran rather than in chloroform, toluene or xylene when the intercalation was conducted in a solvent. When preparing the flexible structured units by solution intercalation, there was no significant impact on the intercalation by the ratio of silicone/OMMT. When preparing the flexible structured units by melt intercalation, the ratio of silicone/OMMT also had little effect on the intercalation.

Investigation by DMA analysis showed that the nanocomposites with intercalated OMMT had a better damping performance than the material with blend OMMT. The presence of LVHS-OMMT improved the damping performance steadily with increasing flexible structure units concentration. The epoxy-nanocomposites with LVPS-OMMT had better damping properties than that with HVHS-OMMT. The free flexible macromolecules in the materials made the glass transition temperature of the epoxy decrease.

Acknowledgments

The authors would like to thank National Natural Science Foundation of China (51273118), Provincial Science and Technology Pillar Program of Sichuan (2013FZ0006), and Program of JPPT-115-5-1716 for financial support, and thank Analytical and Testing Center of Sichuan University for providing XRD, TEM and DMA measurements.

References

- [1] Yamada N, S Shoji. *J Appl Polym Sci*, 1999, 71: 855.
- [2] He T, J. Liu. *Polym Commun*, 1986, 1:30.
- [3] Huang W, F Zhan. *J Appl Polym Sci*, 1995, 50: 277.
- [4] Lee C, Y Wang. *J Polym Sci Polym Chem* 2008, 46: 2262.
- [5] Dhoke SK, S Palraj. *Prog Org Coat*, 2007, 59: 21.
- [6] Fu RQ, JJ Woo. *J Power Sources*, 2008, 179: 458.
- [7] Piscitelli, F, A.M. Scamardella. *J Appl Polym Sci*, 2012, 124: 616.
- [8] Kaynak C, GI Nakas. *Appl Clay Sci*, 2009, 46: 319.
- [9] Ray SS, M Okamoto. *Prog Polym Sci*, 2003, 28: 1539.
- [10] Giannelis EP. *Appl Organomet Chem*, 1998, 12: 675.
- [11] Gilman JW, T Kashiwagi. *Chem Technol Polym Addit*, 1999, 14: 249.
- [12] Ray SS, K Yamada. *Nano Lett*, 2002, 2: 1093.
- [13] Meunier, M; Sheno, R. A. *Compos Struct*, 2001, 243: 54.
- [14] Berthelot J, Assarar M, Sefrani Y, Mahi A. *Compos Struct*, 2008, 85: 189.
- [15] Piscitelli F, P Posocco *J Colloid Interf Sci*, 2010, 351: 108.
- [16] M Fang, Z Zhang, J Li, H Zhang, H Lu and Y Yang. *J Mater Chem*, 2010, 20: 9635.
- [17] Okamoto M, S Morita. *Polymer*, 2000, 41: 3887.
- [18] Okamoto M, S Morita. *Polymer*, 2001, 42: 1201.
- [19] Xu L, H Nakajima. *Macromolecules*, 2009, 42: 3795.
- [20] Xidas PI, KS Triantafyllidis. *Eur Polym J*, 2010, 46: 404.

Captions:

Figure 1: Schematic illustration of damping structure.

(a) rigid layer. (b) damping layer. (c) constrained layer.

Figure 2: XRD patterns of HVHS-SOMMT prepared in different solvents.

(HVHS: SOMMT=3: 1. Temperature: 60°C. Time: 9h.)

Figure 3: XRD patterns of HVHS-OMMT prepared in different solvents.

(HVHS: OMMT=3: 1. Temperature: 60°C. Time: 9h.)

Figure 4: XRD patterns of LVHS-OMMT prepared in different solvents.

(LVHS: OMMT=3: 1. Temperature: 60°C. Time: 9h.)

Figure 5: XRD patterns of HVHS-SOMMT prepared with different weight ratio of HVHS/SOMMT. (Temperature: 60 °C. Time: 9h. Solvent: THF.)

Figure 6: XRD patterns of LVHS-OMMT and LVPS-OMMT prepared by melt intercalation. (Temperature: 60°C. Time: 90min.)

Figure 7: XRD patterns of LVHS-OMMT prepared with different weight ratio of LVHS/OMMT. (Melt intercalation, Temperature: 60°C, Time: 90min.)

Figure 8: TEM image of nanocomposites with a LVHS-OMMT content of 15% in different magnification: (a) 50nm, (b) 100nm. (Melt intercalation, LVHS: OMMT=7: 3, Temperature: 60°C, Time: 90min.)

Figure 9: TEM image of nanocomposites with a LVPS-OMMT content of 15% (Melt intercalation, LVPS: OMMT=7: 3, Temperature: 60°C, Time: 90min.)

Figure 10: DMA curve of two nanocomposites with a LVPS-OMMT content of 10%. (Melt intercalation method, LVPS: OMMT=7: 3, Temperature: 60°C, Time: 90min.)

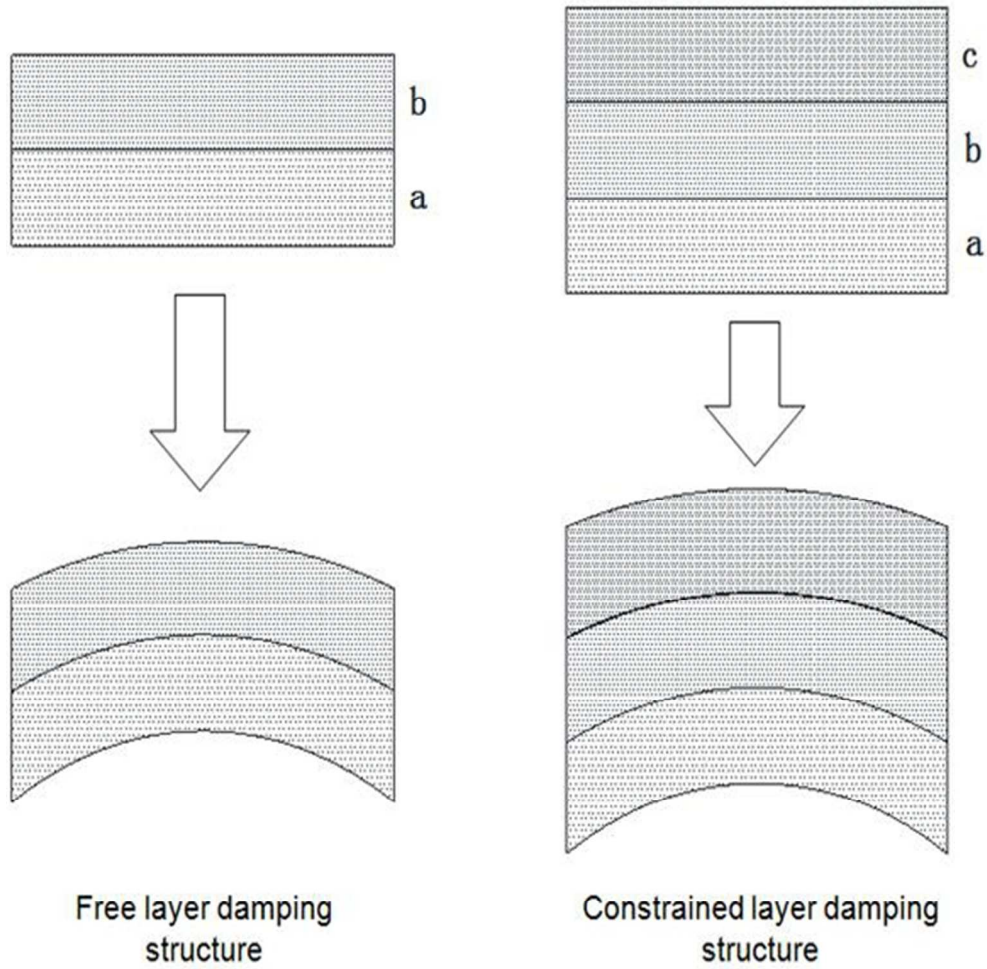
Figure 11: DMA curve of two nanocomposites with a LVHS-OMMT content of 10%. (Melt intercalation, LVHS: OMMT=7: 3. Temperature: 60°C, Time: 90min.)

Figure 12: DMA curve of the nanocomposites with LVPS-OMMT, HVPS-OMMT, LVHS-OMMT and HVHS-OMMT. (LVPS-OMMT (7:3) and LVHS-OMMT (7:3) are prepared by the melt intercalation; HVHS-OMMT (7:3) and HVPS-OMMT (7:3) are prepared by solution intercalation.)

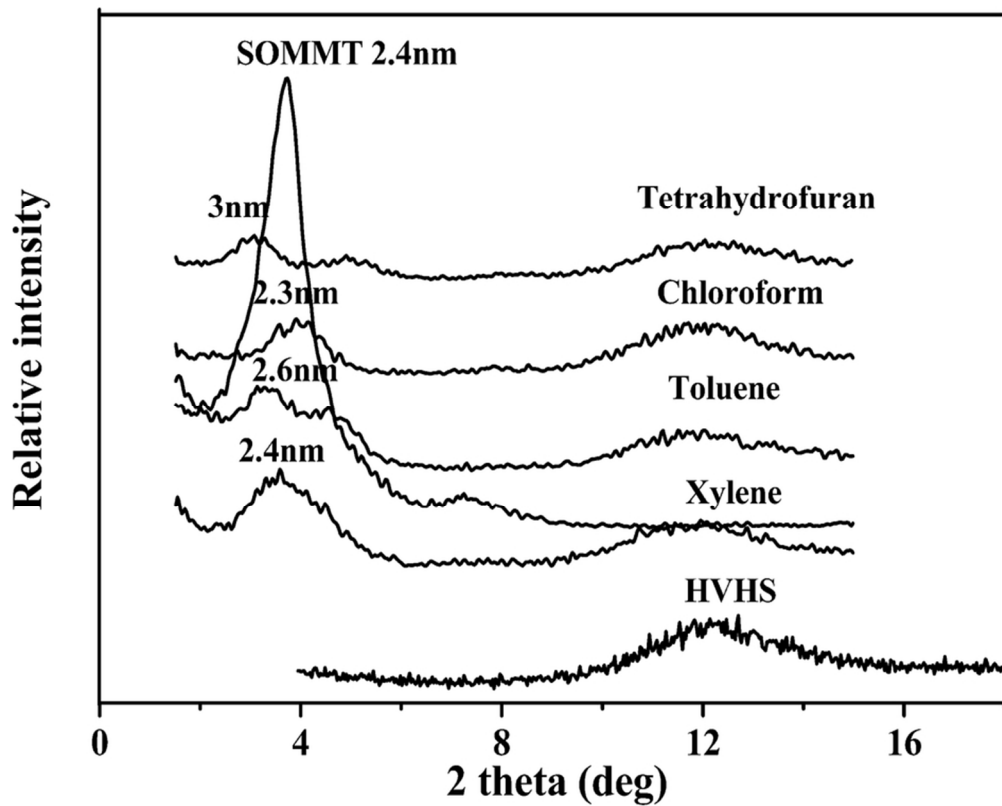
Figure 13: DMA curve of nanocomposites with different LVHS-OMMT content. (Solution intercalation method, LVHS: OMMT=3: 1, Temperature: 60°C, Time: 9h, Solvent: THF.)

Figure 14: DMA curve of two nanocomposites with a LVHS-OMMT content of 15%. (Melt intercalation, Temperature: 60°C, Time: 90min.)

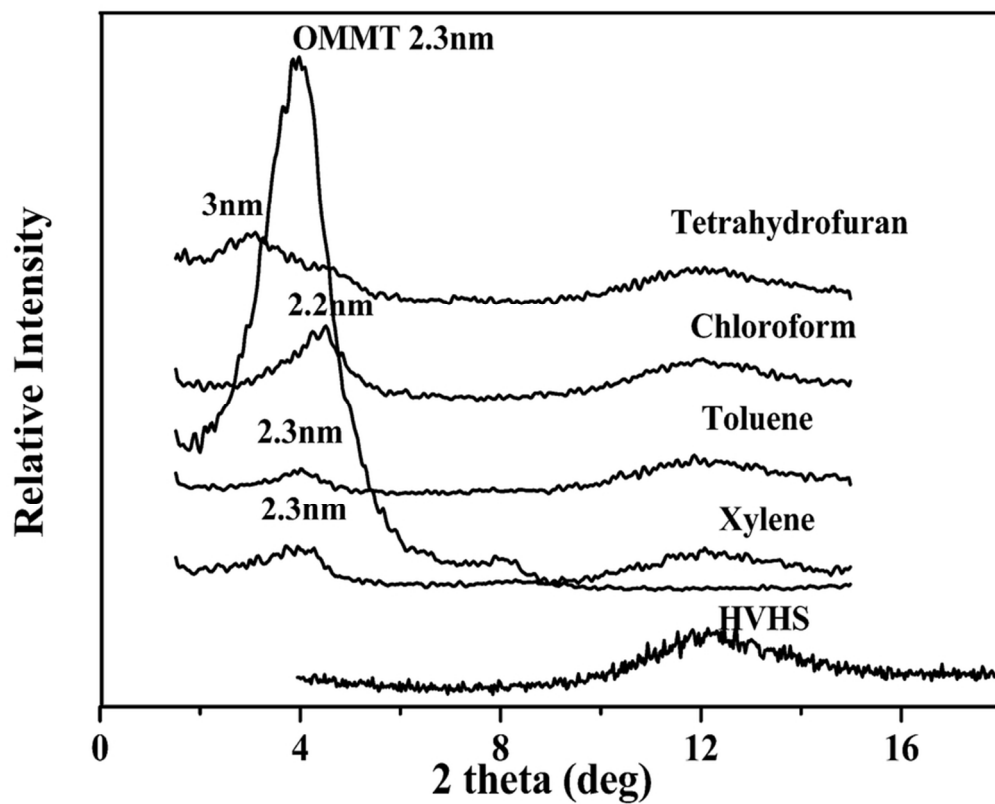
Table 1: Summary of DMA test for various epoxy/OMMT intercalated by silicone macromolecule nanocomposites



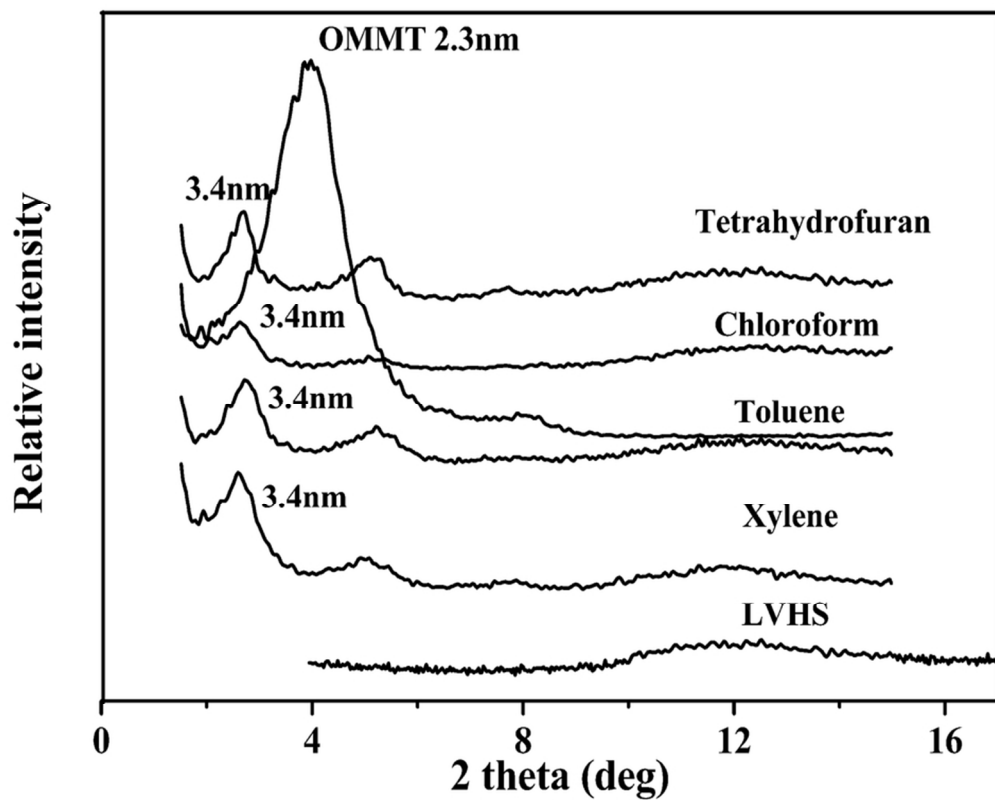
Schematic illustration of damping structure.
(a) rigid layer. (b) damping layer. (c) constrained layer.
50x50mm (300 x 300 DPI)



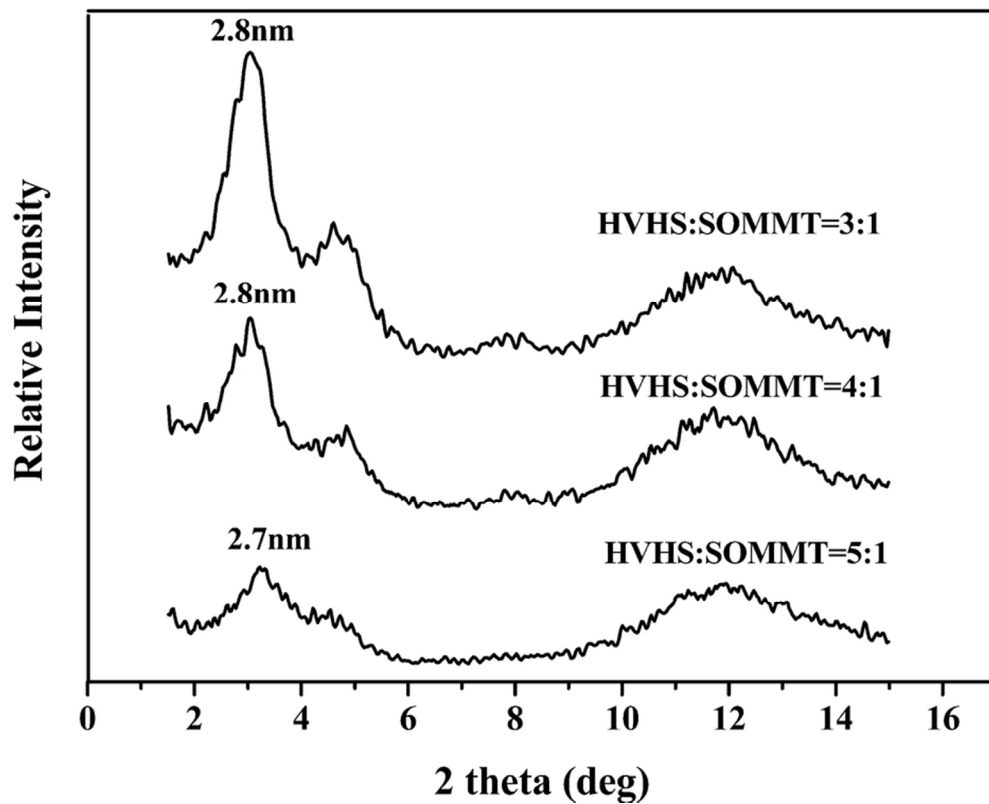
XRD patterns of HVHS-SOMMT prepared in different solvents.
(HVHS: SOMMT=3: 1. Temperature: 60oC. Time: 9h).
40x32mm (600 x 600 DPI)



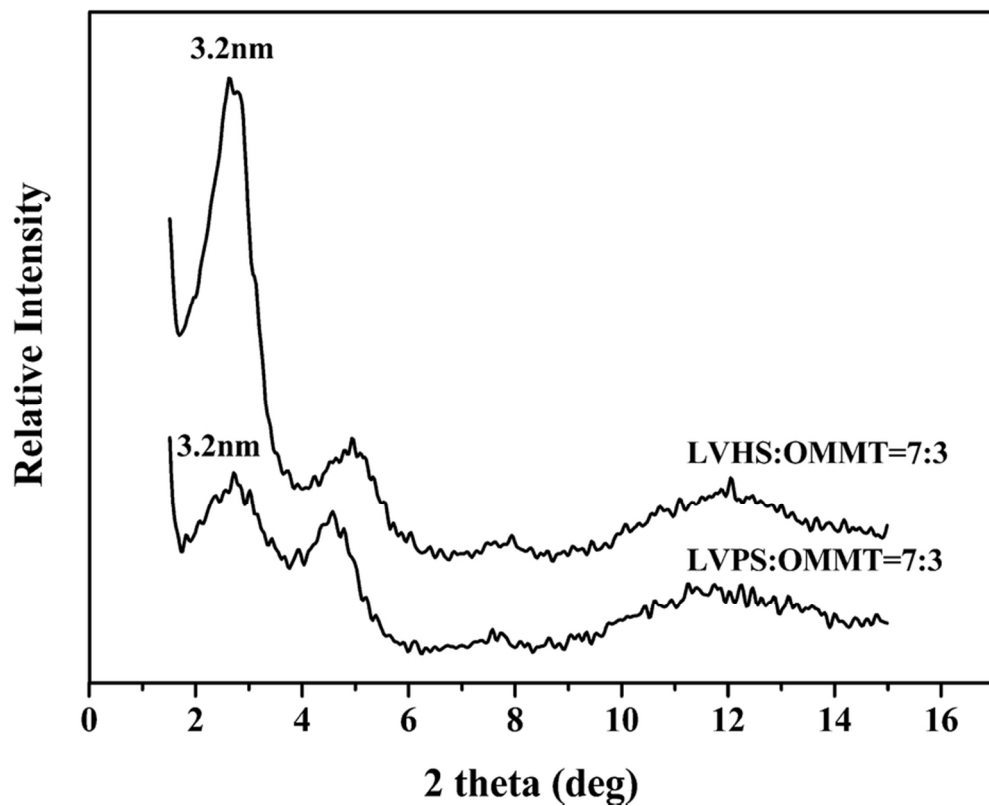
XRD patterns of HVHS-OMMT prepared in different solvents.
(HVHS: OMMT=3: 1. Temperature: 60°C. Time: 9h.)
40x32mm (600 x 600 DPI)



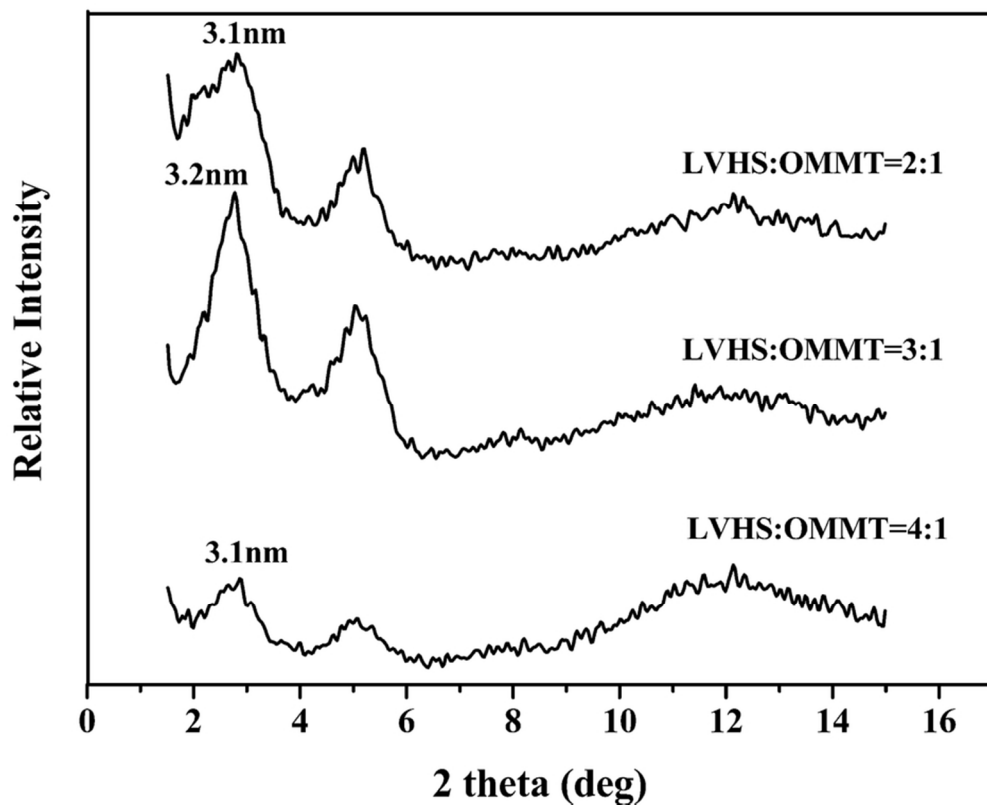
XRD patterns of LVHS-OMMT prepared in different solvents.
(LVHS: OMMT=3: 1. Temperature: 60 oC. Time: 9h.)
40x32mm (600 x 600 DPI)



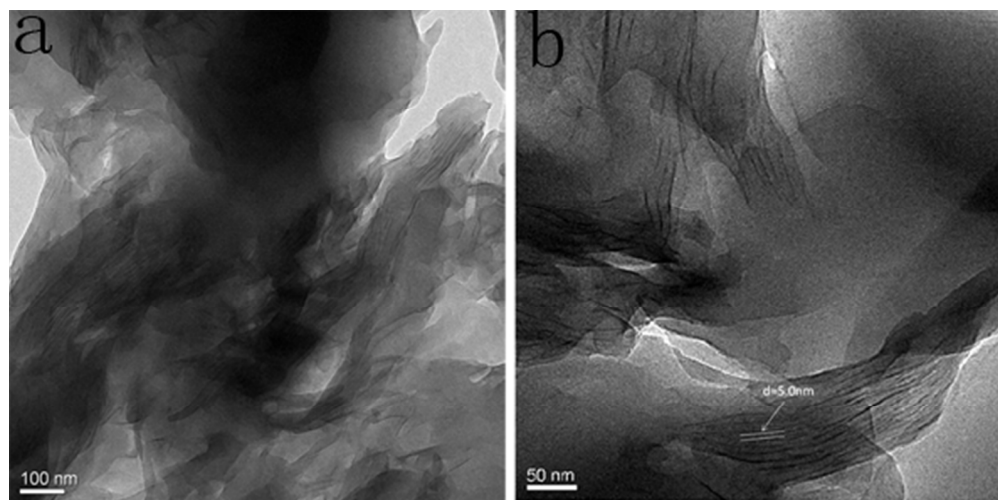
XRD patterns of HVHS-SOMMT prepared with different weight ratio of HVHS/SOMMT. (Temperature: 60 oC.
Time: 9h. Solvent: THF.)
40x32mm (600 x 600 DPI)



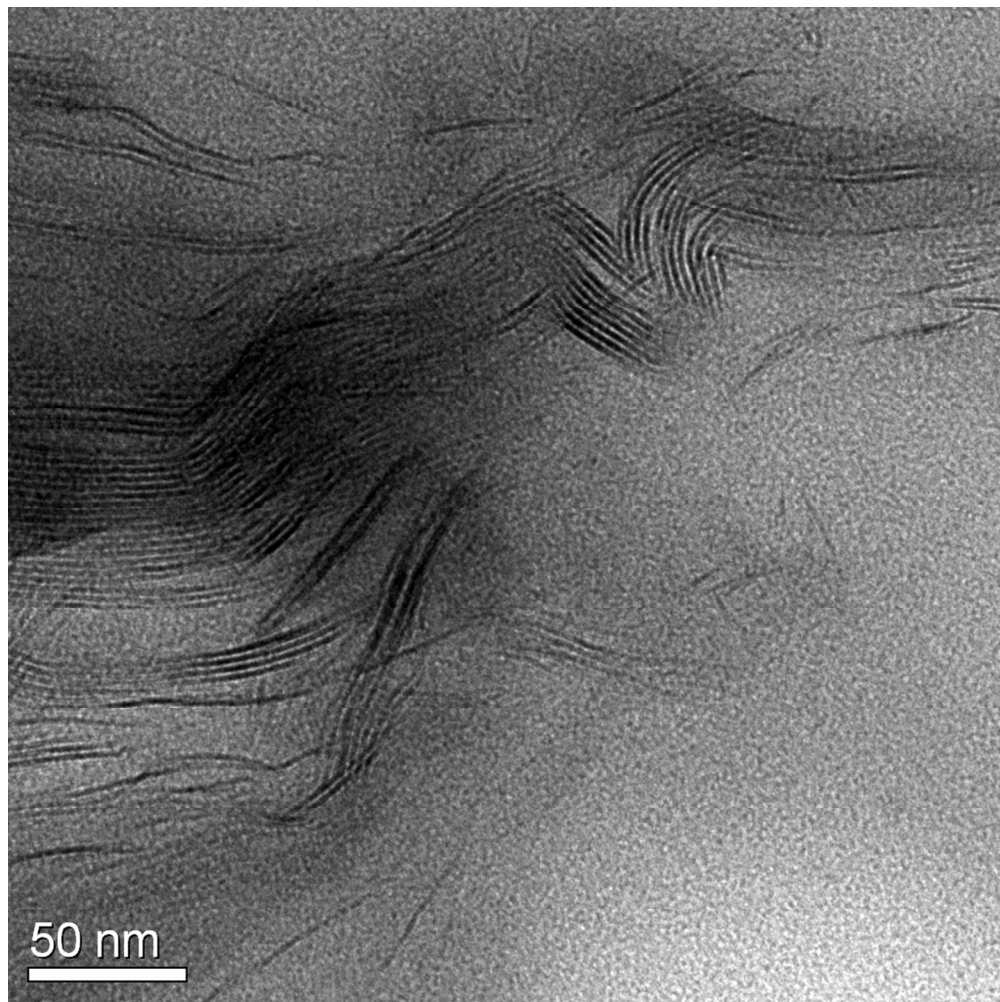
XRD patterns of LVHS-OMMT and LVPS-OMMT prepared by melt intercalation. (Temperature: 60°C. Time: 90 min.)
40x32mm (600 x 600 DPI)



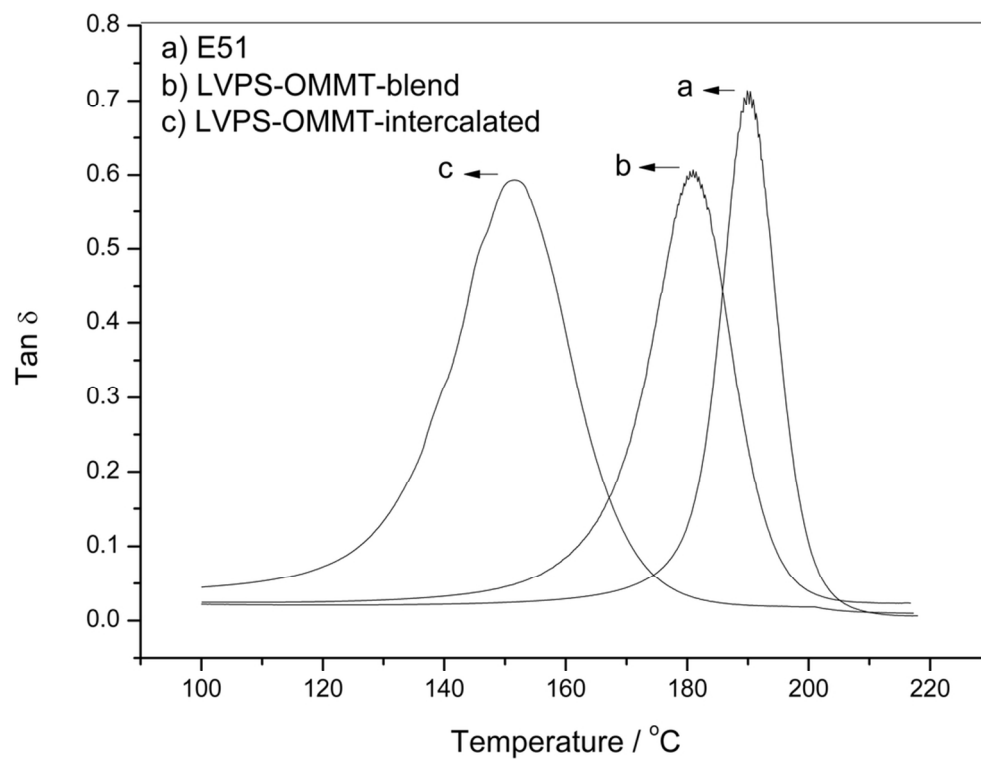
XRD patterns of LVHS-OMMT prepared with different weight ratio of LVHS/OMMT. (Melt intercalation, Temperature: 60°C, Time: 90min.)
40x32mm (600 x 600 DPI)



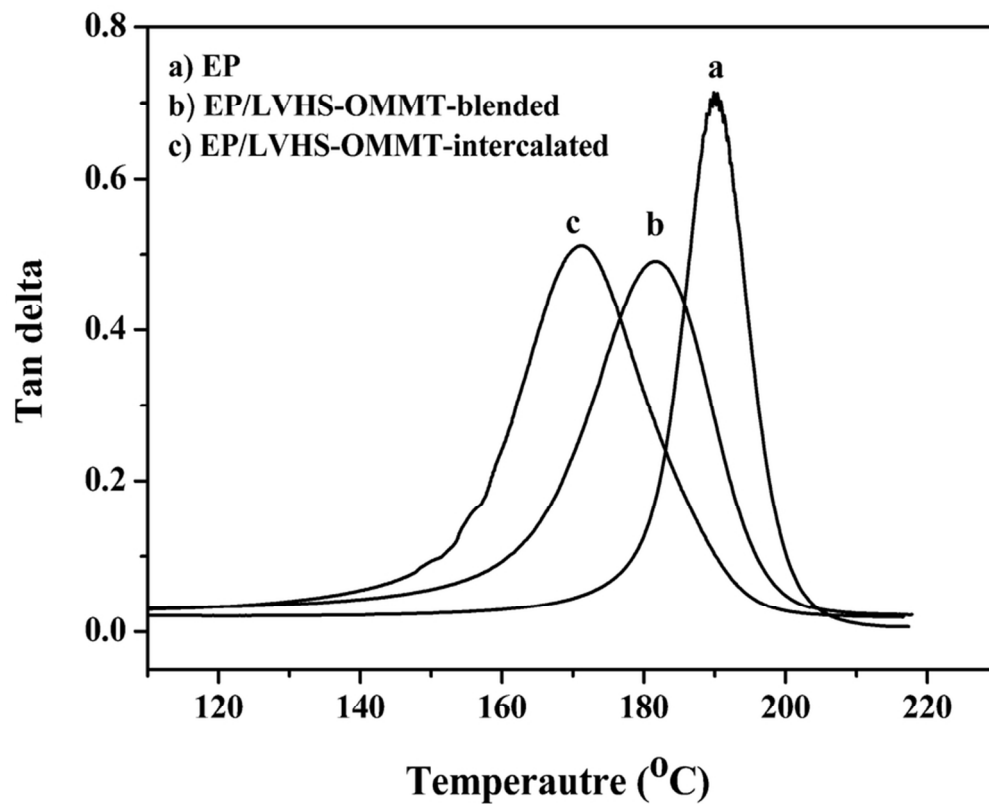
TEM image of nanocomposites with a LVHS-OMMT content of 15% in different magnification: (a) 50nm, (b) 100nm. (Melt intercalation, LVHS: OMMT=7: 3, Temperature: 60oC, Time: 90min.)
50x24mm (300 x 300 DPI)



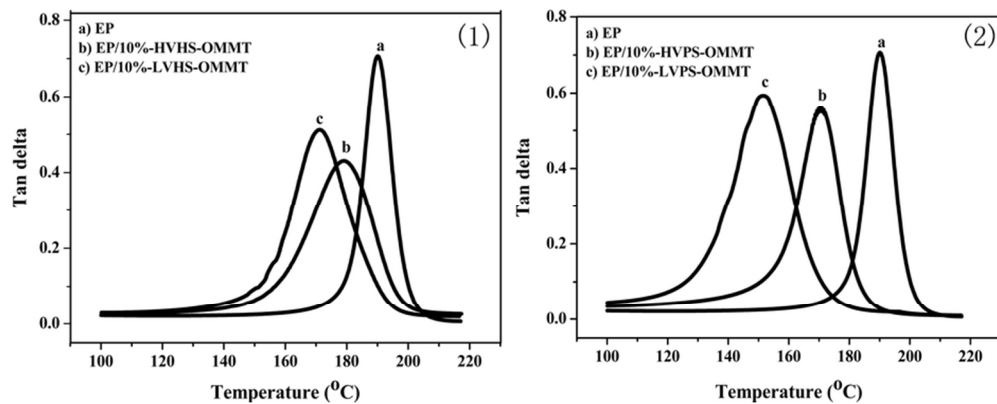
TEM image of nanocomposites with a LVPS-OMMT content of 15% (Melt intercalation, LVPS: OMMT=7: 3, Temperature: 60°C, Time: 90min.)
361x361mm (72 x 72 DPI)



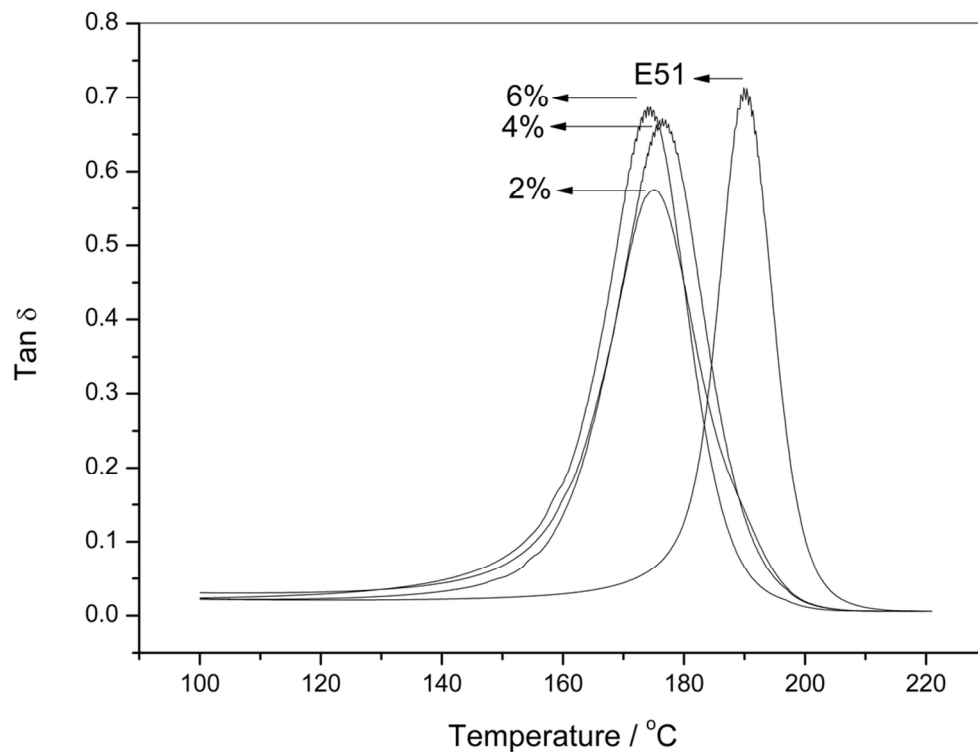
DMA curve of two nanocomposites with a LVPS-OMMT content of 10%.
(Melt intercalation method, LVPS: OMMT=7: 3, Temperature: 60°C, Time: 90min.)
47x35mm (600 x 600 DPI)



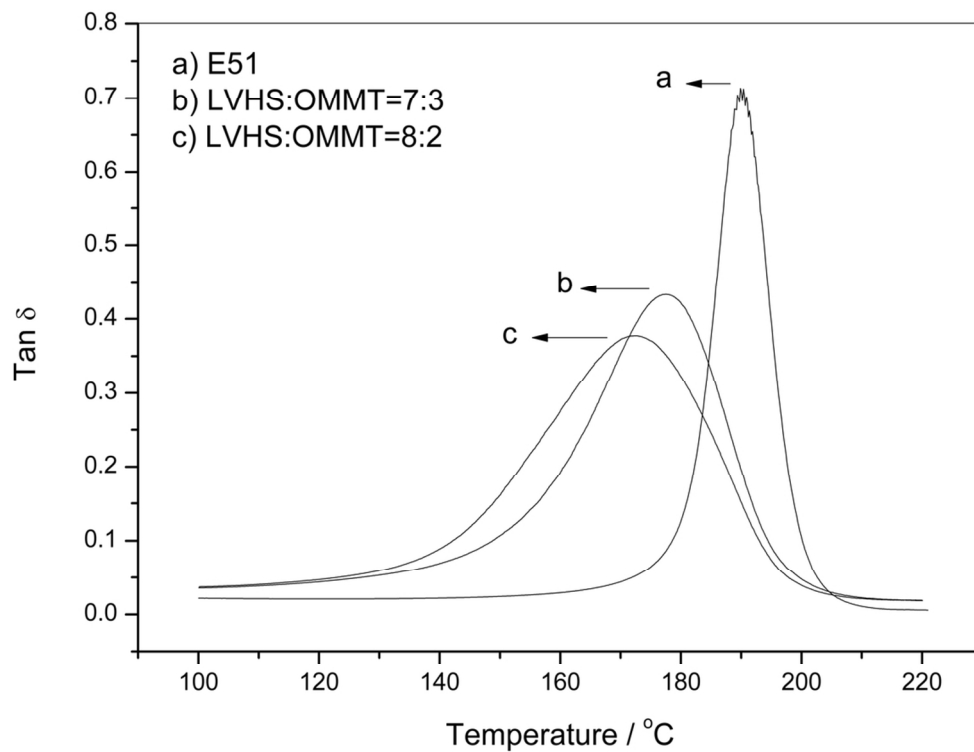
DMA curve of two nanocomposites with a LVHS-OMMT content of 10%.
(Melt intercalation, LVHS: OMMT=7: 3. Temperature: 60oC, Time: 90min.)
40x32mm (600 x 600 DPI)



DMA curve of the nanocomposites with LVPS-OMMT, HVPS-OMMT, LVHS-OMMT and HVHS-OMMT. (LVPS-OMMT (7:3) and LVHS-OMMT (7:3) are prepared by the melt intercalation; HVHS-OMMT (7:3) and HVPS-OMMT (7:3) are prepared by solution intercalation.)
40x15mm (600 x 600 DPI)



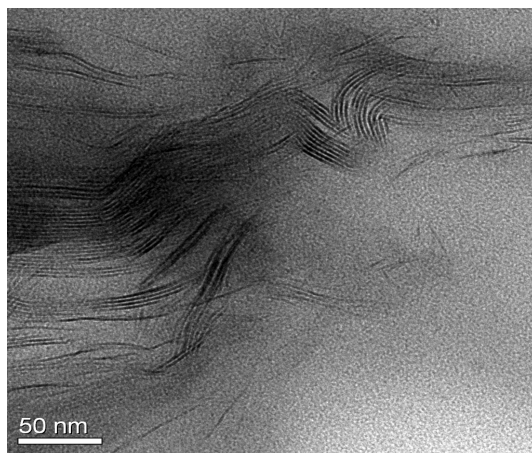
DMA curve of nanocomposites with different LVHS-OMMT content.
(Solution intercalation method, LVHS: OMMT=3: 1, Temperature: 60oC, Time: 9h, Solvent: THF.)
49x37mm (600 x 600 DPI)



DMA curve of two nanocomposites with a LVHS-OMMT content of 15%.
(Melt intercalation, Temperature: 60°C, Time: 90min.)
49x37mm (600 x 600 DPI)

Table 1: Summary of DMA test for various epoxy/OMMT intercalated by silicone macromolecule nanocomposites

Silicone-OMMT Content	Type of silicone	Preparation Method	Silicone : OMMT	Peak area of loss factor
0%	-----	-----	-----	10.87
2%	LVHS	solution	3:1	13.73
4%	LVHS	solution	3:1	15.02
6%	LVHS	solution	3:1	15.07
10%	LVHS	melt	7:3	14.83
10%	LVHS	blend	7:3	13.23
15%	LVHS	melt	7:3	15.70
15%	LVHS	melt	8:2	16.07
10%	LVPS	blend	7:3	13.65
10%	LVPS	melt	7:3	17.63



Flexible silicone macromolecules had been inserted into OMMT and the constrained layer damping structure had been prepared successfully in the nanocomposites.